Cluster-model calculation of the electronic structure of CuO: A model material for the high-T_c superconductors

H. Eskes, L. H. Tjeng, and G. A. Sawatzky
Materials Science Centre, Department of Solid State and Applied Physics, University of Groningen Nijenborgh 18, 9747 AG Groningen, The Netherlands
(Received 6 January 1989)

In this paper we describe the details of several model Hamiltonian cluster calculations, suitable for describing various spectroscopic data of CuO. By treating the *d-d* Coulomb and exchange interactions within the full atomic multiplet theory and using symmetry-dependent Cu-O hybridizations, we do a detailed comparison to photoelectron spectroscopic data, thereby obtaining reliable values for the parameters of an Anderson-model Hamiltonian. We present a study of the allowable ranges of such parameters and a discussion of the applicability to high-T_c copper compounds. For the latter we investigate the influence of the out-of-plane apex oxygen, which is found to be small for the photoelectron spectrum for known Cu-O distances. From a study of the dependence of the nature of the first ionization state on the apex-O–to–Cu distance as well as on the apex-O $2p$ state orbital energy, we determine the values for which this state changes from a singlet to a triplet. However, in all cases this state remains $d^9\underline{L}$ in character. From the parameters obtained for CuO, we derive an O $2p$–Cu $3d$ exchange interaction of 3.4 eV for x^2-y^2 symmetry orbitals. In addition we calculate the energies of the optical *d-d* transitions and find all three of these to be clustered around 1.4±0.1 eV.

I. INTRODUCTION

One of the most basic aspects to be considered, before starting a detailed discussion on the mechanism of superconductivity in the high-T_c copper oxide materials, concerns their electronic structure and more specifically the nature of the states close to the Fermi level. To this end numerous band-structure calculations[1–8] have been done. However, the calculations predict the antiferromagnetic insulating materials to be metallic. These problems are similar to those for the late $3d$ transition-metal oxides,[9,10] which since 1937 have been known to be a result of the breakdown of the one-electron band theory description[11] due to the strong *d-d* Coulomb and exchange interactions.[12,13] Recently Ghijsen *et al.*[14] demonstrated that band-structure calculations give good results for Cu_2O, but have severe shortcomings for CuO.

Better approaches to describe the electronic structure of these systems are for instance impurity and cluster configuration interaction[15–19] model calculations. In such calculations part or all of the translational symmetry is neglected in favor of a then possible explicit treatment of local on-site electron-electron interactions. Assuming, as is generally accepted, that superconductivity in the high-T_c materials takes place in the CuO_2 planes, one then studies a Cu impurity in an O band or a cluster of the type $(CuO_4)^{6-}$, $(CuO_5)^{8-}$, or $(CuO_6)^{10-}$, respectively.[20–25] Values for the model parameters used are to be determined from experiments and/or *ab initio* calculations. However, comparison of the results of the calculations to, for instance, valence-band photoelectron-spectroscopy data, are hampered by the fact that these data depend strongly on the exact chemical composition and sample preparation treatment:[26–41] Not only are other elements like La-Sr, Y-Ba, Eu-Ba, and Bi-Ca-Sr or contaminants present, but also the oxygen content and the crystal structure on the surface might be different from that of the bulk. A somewhat better consistency exists for Cu $2p$ core-level spectroscopy data[42–48] and Cu $3p$ resonant photoemission data,[35,49,50] but these contain only limited information. It is difficult to obtain reliable values for the model parameters used from high-T_c data. We therefore choose to study the electronic structure of CuO, for which well-defined core level, (resonant) valence-band, and inverse photoemission, as well as x-ray absorption data, are available.[14,51,52]

There is a large number of similarities between CuO and the high-T_c compounds which makes it possible to consider CuO as a model material for the high-T_c compounds. The energy gap of CuO (1.4 eV) (Refs. 14 and 53) is close to that of the insulating high-T_c compounds (1.5–2.0 eV). This indicates that the on-site energy difference between the Cu $3d$ and O $2p$ states for both compounds is quite similar, consistent with Madelung potential calculations.[54] The Cu $2p$ core level spectra indicate the presence of primarily Cu^{2+} in both compounds. Valence-band resonant photoemission on the Cu $3p$ edge reveals the presence of d^8 final states at comparable binding energies. Therefore the *d-d* Coulomb interactions will be of the same magnitude. Turning to the crystal structure,[55] we will describe CuO in terms of a $(CuO_4)^{6-}$ cluster in D_{4h} symmetry, neglecting the fact that the O—Cu—O angle in the actual lattice is 84° rather than 90°. The Cu–O distance is 1.95 Å. This cluster is also the basic structural unit of the CuO_2 planes of the high-T_c compounds, having comparable Cu–O distances: 1.89 Å

for the La-Sr and 1.96 Å for the Y-Ba copper oxide compounds. This indicates also that the transfer integrals and hybridizations are comparable. In addition, neutron-diffraction[56–59] and two magnon Raman[60] data of La_2CuO_4 and CuO yield similar values for the Cu—O—Cu antiferromagnetic superexchange interaction: 0.12 eV and 0.09 eV, respectively. This difference is well explained by the difference in the Cu—O—Cu bond angles θ, being 180° and 146°, respectively, and the well-known $\cos^2\theta$ dependence of the superexchange interaction.[61–63] Since the charge-transfer energy, the *d-d* Coulomb interaction, and the transfer integrals determine the superexchange interaction, this again strongly suggests similar values for these parameters.

Of course, besides these similarities there are also differences. In the high-T_c compounds, there are in the neighborhood, out of the plane of the basic structural unit mentioned above, one (Y-Ba, Eu-Ba, Bi-Sr-Ca compounds) or two (La-Sr compounds) other oxygen ions present, forming a pyramidal $(CuO_5)^{8-}$ or a distorted octahedral $(CuO_6)^{10-}$ cluster. Another difference to be considered is the way in which the clusters are linked together. In CuO the clusters are connected via their sides to form a ribbon, whereas for the high-T_c compounds the clusters are connected via each of their corners to form a plane. This might cause some differences in polarization and screening effects in the lattice, and therefore also some differences in the values of the model parameters.

Our cluster model includes ligand field splitting and treats exactly the *d-d* Coulomb and exchange interactions within the full atomic multiplet theory using screened atomic Racah parameters.[64,65] It is generally found for transition and rare-earth metals and their compounds that the multiplet splitting is almost the same as for the free ions although the monopole part of the Coulomb interactions is strongly screened.[66]

We perform here a model calculation rather than an *ab initio* cluster calculation for the following reasons. *Ab initio* calculations, using almost exact Madelung potentials due to distant ions, generally yield a much too large band gap: 10 eV for NiO,[67] and 12 eV for Si.[68] Janssen and Nieuwpoort[67] have shown that this is most likely due to more distant polarizable ions outside the cluster. In NiO this results in strongly overestimated *d-d* Coulomb interactions and charge-transfer energies. Until now, no satisfactory method has as yet been found for taking into account these screening and polarization effects in a self-consistent way.

It is interesting to compare our cluster calculation with an impurity approach.[22,23] In the impurity case the O 2*p* host states form a band, while for the cluster the large oxygen-oxygen hybridization is only included via the difference in energy for the different symmetry levels. An advantage of the cluster model is that these levels are shifted upon copper-oxygen hybridization. In the impurity approach, the effect on the rigid oxygen band is only noticed if the impurity-host hybridization is large enough to create bound states. Furthermore, questions concerning the character of the wave functions are easily obtained in the cluster case, while they involve integrations over energy in the impurity case.

It is interesting to note that the first ionization states of, for instance, insulating La_2CuO_4 and $YBa_2Cu_3O_6$ would be the holes present in doped and superconducting $La_{2-x}Sr_xCuO_4$ and $YBa_2Cu_3O_{7-y}$ ($y<0.5$). There are strong spectroscopic indications that these states are of primarily O 2*p* character in the doped materials.[31,69–73] This would put the insulators in the *B* (charge-transfer gap) region of the Zaanen-Sawatzky-Allen[18] (ZSA) diagram and would move towards region *D* (ligand hole conduction) upon substitution. It also implies that the Cu 3*d*-3*d* Coulomb and exchange interactions are larger than the O 2*p*–Cu 3*d* charge-transfer energy, as was already predicted for CuO in the original ZSA article of 1985. The extra ligand holes would then be responsible for conduction in the high-T_c compounds. In this regard we pay special attention to the lowest-energy state near the Fermi level, which is found to have a singlet character ($^1A_1$).[23] To verify if out-of-plane oxygen atoms in the high-T_c compounds can influence this result, we extend the calculations to a $(CuO_6)^{10-}$ cluster.

II. THEORY

The objective of the cluster-model calculation is to obtain (a) the Cu 3*d*, the O 2*p*, and the total electron removal spectral weight, to be compared with valence-band photoemission spectra; (b) the Cu $3d^8$ partial density of states (DOS), which is required to interpret valence-band Cu 3*p* resonant photoemission spectra; (c) the Cu 3*d* and O 2*p* partial DOS in the one-particle approximation which are compared with results from band-structure calculations; (d) the band gap $E_{\rm gap}$, which is defined as the energy required to remove an electron from the first ionization state plus the energy required to return the electron to the first affinity state; (e) the ground-state hybridization energy δ and the average Cu 3*d* hole occupation $\langle n_d \rangle$; (f) the character (symmetry, spin, and orbital composition) of the first ionization state; (g) the Cu 3*d* ligand field splitting and the energies of the optical *d-d* and charge-transfer transitions.

The model calculation includes the Cu 3*d*–Cu 3*d* Coulomb and exchange interactions using the full atomic multiplet theory. The model Hamiltonian is given by

$$H = H_0 + H_1 \tag{1}$$

$$H_0 = \sum_m \varepsilon_d(m) d_m^\dagger d_m + \sum_m \varepsilon_p(m) p_m^\dagger p_m + \sum_m T_{pd}(m)(d_m^\dagger p_m + p_m^\dagger d_m) \tag{2}$$

$$H_1 = \sum_{m,m',n,n'} U(m,m',n,n') d_m^\dagger d_{m'} d_n^\dagger d_{n'} . \tag{3}$$

Here the operator $d_m^\dagger$ creates a Cu 3*d* hole with energy $\varepsilon_d(m)$ and the operator $p_m^\dagger$ a hole in the ligand O 2*p* orbitals with energy $\varepsilon_p(m)$. The oxygen-oxygen hybridization is already included. $T_{dp}(m)$ is the transfer integral for the Cu 3*d*–O 2*p* ligand hybridization. The indices m, m', n, and n' denote orbital and spin quantum numbers. The energies $\varepsilon_d(m)$, $\varepsilon_p(m)$, and the integrals $T_{pd}(m)$ do not depend on spin. H_0 describes the one-particle hy-

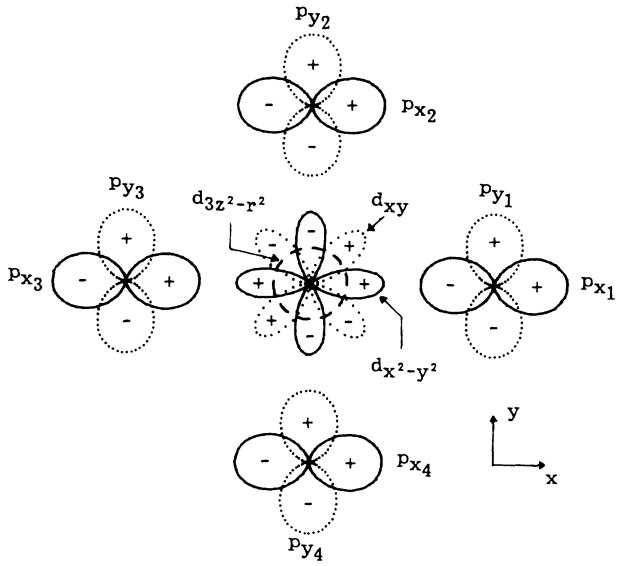

FIG. 1. Orbitals used in the $(CuO_4)^{6-}$ cluster calculation. The z direction points towards the reader. The O $2p_z$ and Cu $3d_{xz}, 3d_{yz}$ orbitals are not drawn.

bridization between the Cu $3d$ states and the ligand orbitals, and H_1 describes the two-particle Cu $3d$ Coulomb and exchange interactions U. In this Hamiltonian we have neglected all the core levels and even more important the Cu $4s,4p$ as well as the empty O bands. These are quite high in energy and therefore we assume that their influence via hybridization, etc., can be treated as a renormalization of the effective parameters. The ground state is given by one hole in otherwise closed Cu $3d$ and O $2p$ shells. A photoemission experiment will result in a two-hole problem $(CuO_4)^{5-}$, which is exactly solvable and an inverse photoemission experiment will bring us to the closed-shell configuration.

With the $(CuO_4)^{6-}$ cluster in square planar symmetry, the quantum numbers m are, aside from spin, conveniently taken to be the b_1 $(d_{x^2-y^2})$, a_1 $(d_{3z^2-r^2})$, b_2 (d_{xy}), and e (d_{xz},d_{yz}) orbitals, which are the gerade irreducible representations spanned by a d-hole in a D_{4h} point group. The ligand hole wave functions consist of linear combinations of O $2p$ orbitals with the above symmetries. Figure 1 shows the orbitals used. The nonbonding ligand hole wave functions are not included as they can be considered as bonding with the Cu $3d$ states of neighboring clusters. Also note that these do not appear in the ground state and the Cu $3d$ electron removal spectrum. Omitting the point-charge crystal-field splitting, thought to be less than 1 eV, the on-site d-hole energy is independent of m, and is set to zero. The energy of all unhybridized O $2p$ states is then the charge-transfer energy Δ_{pd}. Due to nearest-neighbor O $2p$–O $2p$ hybridization, the effective charge-transfer energy is, for instance for the b_1-symmetry ligand hole, lowered to $\Delta_{pd}-T_{pp}$, where T_{pp} includes both σ and π bonding $[T_{pp}=(pp\sigma)-(pp\pi)]$. Following Slater and Koster[74] we have $T_{pd}(a_1)=T_{pd}(b_1)/\sqrt{3}=(pd\sigma)$ and $T_{pd}(e)=T_{pd}(b_2)/\sqrt{2}=\sqrt{2}(pd\pi)$. As in general $(pd\pi)$ is somewhat less than $(pd\sigma)/2$,[75] we take $T_{pd}(b_2)=T_{pd}(b_1)/2$. Note that as long as $T_{pd}(a_1)\ll T_{pd}(b_1)$, a change in the ratio between these parameters will not influence the final results very much. These differences in $T_{pd}(m)$ yield the ligand field splitting. Table I lists all irreducible representations, basis functions, and matrix elements of the one-hole problem.

For each symmetry (m), the solution to the one-hole problem is obtained by diagonalizing a 2×2 matrix, yielding bonding (a) and antibonding (b) type orbitals in terms of which the Hamiltonian is

$$H_0=\sum_m \varepsilon_a(m)a_m^\dagger a_m+\sum_m \varepsilon_b(m)b_m^\dagger b_m \tag{4}$$

$$a_m=\alpha_m d_m+\beta_m p_m \tag{5}$$

$$b_m=\beta_m^* d_m-\alpha_m^* p_m\ . \tag{6}$$

TABLE I. Irreducible representation (all gerade), one-hole basis functions, and matrix elements for the $(CuO_4)^{6-}$ cluster in D_{4h} symmetry. The nonbonding ligand O $2p$ orbitals are not included.

Irreducible representations m	Cu $3d$ basis d_m	O $2p$ basis p_m
a_1	$d_{3z^2-r^2}$	$(1/\sqrt{4})(p_{x_1}+p_{y_2}-p_{x_3}-p_{y_4})$
b_1	$d_{x^2-y^2}$	$(1/\sqrt{4})(p_{x_1}-p_{y_2}-p_{x_3}+p_{y_4})$
b_2	d_{xy}	$(1/\sqrt{4})(p_{y_1}+p_{x_2}-p_{y_3}-p_{x_4})$
e	d_{xz},d_{yz}	$(1/\sqrt{2})(p_{z_1}-p_{z_3}),(1/\sqrt{2})(p_{z_2}-p_{z_4})$

Irreducible representations	Matrix elements $\langle p_{x_1}\|H\|p_{x_1}\rangle=\Delta_{pd}$, $\langle p_{x_1}\|H\|p_{y_2}\rangle=\frac{1}{2}T_{pp}$		
m	$\varepsilon_d(m)=\langle d_m\|H\|d_m\rangle$	$\varepsilon_p(m)=\langle p_m\|H\|p_m\rangle$	$T_{pd}(m)=\langle p_m\|H\|d_m\rangle$
a_1	0	$\Delta_{pd}+T_{pp}$	$T_{pd}(b_1)/\sqrt{3}$
b_1	0	$\Delta_{pd}-T_{pp}$	$T_{pd}(b_1)$
b_2	0	$\Delta_{pd}+T_{pp}$	$T_{pd}(b_1)/2$
e	0	Δ_{pd}	$T_{pd}(b_1)/2\sqrt{2}$

Because of the large hybridization, the ground state (g.s.) is that with one hole in an orbital of b_1 symmetry

$$|\psi_{\text{g.s.}}\rangle = a^{\dagger}_{b_1\uparrow}|0\rangle \tag{7}$$

where $|0\rangle$ is the state with a closed ligand O $2p$ shell and Cu in a d^{10} configuration. The spin of the hole is arbitrarily taken to be up. The ground-state hybridization energy δ is

$$\delta = \tfrac{1}{2}(\Delta_{pd} - T_{pp}) - [T^2_{pd}(b_1) + \tfrac{1}{4}(\Delta_{pd} - T_{pp})^2]^{1/2} . \tag{8}$$

The average ground-state Cu $3d$ hole occupation $\langle n_d \rangle$ is

$$\langle n_d \rangle = a_{b_1\uparrow} a^{*}_{b_1\uparrow} = [1 + \delta^2 / T^2_{pd}(b_1)]^{-1} . \tag{9}$$

Figure 2 shows the energy-level scheme of the one-hole basis functions, using parameter values listed in Table II for $E_{\text{gap}} = 1.8$ eV. This scheme also gives the energies for the forbidden local d-d transitions starting from the ground state.

In a photoemission experiment we have to deal with the propagation of an extra hole put into the ground state with one hole already present. The d and p spectral weight as well as the d^8 partial DOS are given by

$$\rho^{<}_d(E) = \sum_{m,m'} \lim_{\eta \downarrow 0} \frac{1}{\pi} \text{Im} G^{<}_{dd}(m,m',E - i\eta) \tag{10}$$

$$\rho^{<}_p(E) = \sum_{m,m'} \lim_{\eta \downarrow 0} \frac{1}{\pi} \text{Im} G^{<}_{pp}(m,m',E - i\eta) \tag{11}$$

$$\rho^{<}_{d^8}(E) = \sum_{m,m'} \lim_{\eta \downarrow 0} \frac{1}{\pi} \text{Im} G^{<}_{d^8}(m,m',E - i\eta) \tag{12}$$

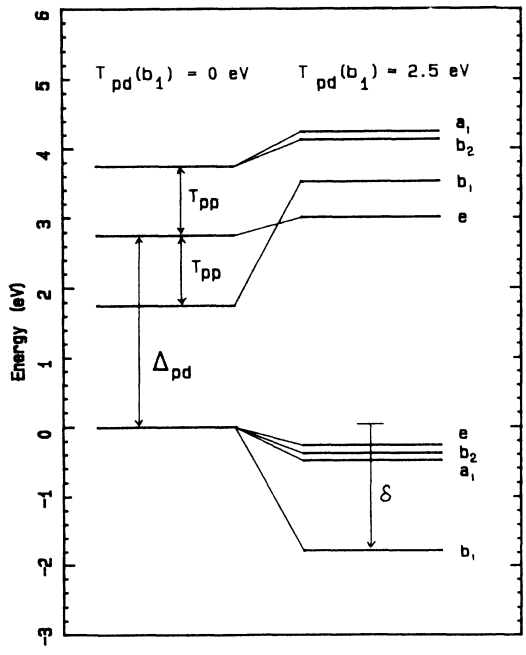

FIG. 2. Energy-level scheme of the one-hole basis functions before and after Cu $3d$–O $2p$-ligand hybridization. The functions and parameters are defined in Table I. The energy levels are drawn for parameter values listed in Table II for $E_{\text{gap}} = 1.8$ eV.

TABLE II. Parameter values used in the cluster-model calculations. The calculation input is Δ_{pd}, $T_{pd}(b_1)$, and T_{pp} as defined in Table I; the Racah A, B, and C parameters as used in Table III; and the lifetime and experimental broadening factor η (FWHM $= 2 \rightarrow 4\eta$). The output includes the valence-band–conduction-band energy gap E_{gap}, the ground-state hybridization energy δ, and the average ground-state Cu $3d$ hole occupation $\langle n_d \rangle$.

	$E_{\text{gap}} = 1.2$ eV	$E_{\text{gap}} = 1.8$ eV	$E_{\text{gap}} = 2.4$ eV
Δ_{pd}	2.2 eV	2.75 eV	3.5 eV
T_{pd}	2.3 eV	2.5 eV	3.0 eV
T_{pp}	1.25 eV	1.0 eV	0.5 eV
A	6.0 eV	6.5 eV	7.0 eV
B	0.15 eV	0.15 eV	0.15 eV
C	0.58 eV	0.58 eV	0.58 eV
η	0.4 eV	0.4 eV	0.4 eV
δ	−1.87 eV	−1.77 eV	−1.85 eV
$\langle n_d \rangle$	0.601	0.665	0.724

with

$$G^{<}_{dd}(m,m',z) = \langle \psi_{\text{g.s.}} | d_{m'} G(z) d^{\dagger}_m | \psi_{\text{g.s.}} \rangle \tag{13}$$

$$G^{<}_{pp}(m,m',z) = \langle \psi_{\text{g.s.}} | p_{m'} G(z) p^{\dagger}_m | \psi_{\text{g.s.}} \rangle \tag{14}$$

$$G^{<}_{d^8}(m,n,z) = \langle 0 | d_n d_m G(z) d^{\dagger}_m d^{\dagger}_n | 0 \rangle \tag{15}$$

$$G(z) = (z + \delta - H)^{-1}, \quad z = E - i\eta \tag{16}$$

in which the d^8 partial DOS is convenient for describing resonant photoemission. The total spectral weight is the sum of the d and p spectral weights normalized to $10 - \langle n_d \rangle$ and $5 + \langle n_d \rangle$ electrons, respectively.

The d-d Coulomb and exchange interactions can be defined in terms of the Racah A, B, and C parameters.[64,65] The d^8 states span singlet and triplet irreducible representations in D_{4h} for which the Coulomb and exchange matrix elements $U(m,m',n,n')$ and basis functions[19] are given in Table III. The above-mentioned expressions could be solved by diagonalizing the matrices in terms of two-hole basis functions, followed by the required projection operations. Equivalently, the more direct Green's-function method could be used. Here we choose for the last method and details of the calculations are presented in the Appendix.

III. RESULTS AND DISCUSSION

We treat four parameters as free variables. These are the on-site copper-to-oxygen charge-transfer energy Δ_{pd}, the copper-oxygen charge-transfer integral for the b_1-symmetry $T_{pd}(b_1)$, the oxygen-oxygen charge-transfer integral T_{pp}, which is $\frac{1}{4}$ of the total oxygen bandwidth, and the Racah A parameter, which is the monopole part of the d-d Coulomb interaction. The parameters are varied under the constraint that the calculated energy gap is 1.8 eV, somewhat larger than the experimental value of 1.4 eV,[14,53] in order to include a dispersional broadening due to translational symmetry. For the Racah B and C parameters we use the free-ion optical values of 0.15 eV and

TABLE III. Irreducible representations spanned by two d holes (d^8) and Coulomb and exchange matrix elements in terms of the Racah A, B, and C parameters.

$^1A_2$	b_1b_2		$^3B_1$	a_1b_1		$^3B_2$	a_1b_2	
b_1b_2	$A+4B+2C$		a_1b_1	$A-8B$		a_1b_2	$A-8B$	
$^3A_2$	b_1b_2	e^2	$^1B_1$	a_1b_1	e^2	$^1B_2$	a_1b_2	e^2
b_1b_2	$A+4B$	$6B$	a_1b_1	$A+2C$	$-2B\sqrt{3}$	a_1b_2	$A+2C$	$-2B\sqrt{3}$
e^2	$6B$	$A-5B$	e^2	$-2B\sqrt{3}$	$A+B+2C$	e^2	$-2B\sqrt{3}$	$A+B+2C$

^3E	eb_1	ea_1	eb_2	^1E	eb_1	ea_1	eb_2
eb_1	$A-5B$	$-3B\sqrt{3}$	$3B$	eb_1	$A+B+2C$	$-B\sqrt{3}$	$-3B$
ea_1	$-3B\sqrt{3}$	$A+B$	$-3B\sqrt{3}$	ea_1	$-B\sqrt{3}$	$A+3B+2C$	$-B\sqrt{3}$
eb_2	$3B$	$-3B\sqrt{3}$	$A-5B$	eb_2	$-3B$	$-B/\sqrt{3}$	$A+B+2C$

$^1A_1$	a_1^2	b_1^2	b_2^2	e^2
a_1^2	$A+4B+3C$	$4B+C$	$4B+C$	$(B+C)\sqrt{2}$
b_1^2	$4B+C$	$A+4B+3C$	C	$(3B+C)\sqrt{2}$
b_2^2	$4B+C$	C	$A+4B+3C$	$(3B+C)\sqrt{2}$
e^2	$(B+C)\sqrt{2}$	$(3B+C)\sqrt{2}$	$(3B+C)\sqrt{2}$	$A+7B+4C$

0.58 eV,[76] respectively, since screening in the solid state occurs primarily for the monopole part of the Coulomb interaction.[66] A Lorentzian experimental broadening of $4\eta=1.6$ eV (full width at half maximum—FWHM) is take into account. No energy-dependent lifetime broadening is included.

A. Valence-band photoemission

The experimental photoemission spectra at photon energies of 21.2 eV (He I), 40.8 eV (He II), and 1486.6 eV (XPS, Al $K\alpha$), are shown in Fig. 3. The theoretical total and Cu $3d$ spectral weight, which are calculated with the cluster model using the same parameter values as in Fig. 2 and listed in Table II for $E_{\rm gap}=1.8$ eV, are also displayed in Fig. 3. The known dependence of the photoionization cross-section ratio upon the photon energy enables us to identify regions of primarily O $2p$ or Cu $3d$ spectral weight. The cross-section ratios, weighted by the number of electrons per atom, are $\sigma(\text{O } 2p)/\sigma(\text{Cu } 3d)\approx 2.16$, 1.05, and 0.03 for He I, He II, and XPS light sources, respectively.[77] Therefore, in XPS we have primarily d emission, to be compared with the calculated d spectral weight, where as in He I and He II spectra we see more or less equally both the d and p emission, to be compared with the calculated total spectral weight.

An analysis of the character of the eigenstates shows that the $d^9\underline{L}$ final states are concentrated in the low-energy structure (containing peak B, shoulders A and C), the $d^{10}\underline{L}^2$ final states in the region around peaks D_1 and D_2, and the d^8 final states at higher energies (containing peaks D_1, D_2, E, and F) ($\underline{L}$ denotes a ligand hole). The large range of the spectral distribution indicates strong (multiplet dependent) Coulomb interactions. The fact that the d^8 final states are at higher binding energies than the $d^9\underline{L}$ final states shows that the Coulomb interaction energies are larger than the charge-transfer energy.

To obtain parameter values we rely mostly on the XPS spectrum, where we can restrict ourselves to d emission. We expect that our calculations are more accurate for the copper than the oxygen spectral weight because the nearest-neighbor coordination of copper is taken into account properly. Furthermore for XPS the sudden ap-

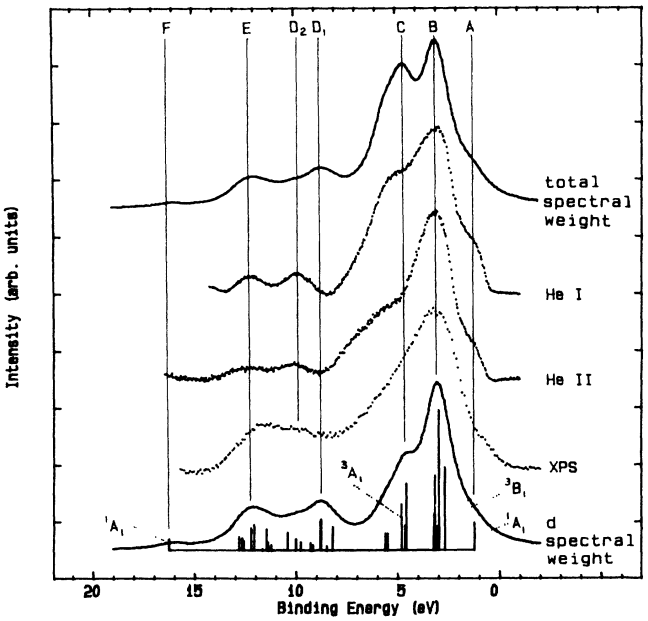

FIG. 3. Valence-band photoemission spectrum of CuO, normalized to the peak height. The dotted lines show the experimental spectra using He I (21.2 eV), He II (40.8 eV), and Al $K\alpha$ (1486.6 eV, XPS) sources. The top solid line shows the calculated total spectral weight and the bottom solid line the calculated Cu $3d$ spectral weight, using the cluster-model theory with parameter values as in Fig. 2 and listed in Table II for $E_{\rm gap}=1.8$ eV. Also shown are the unbroadened states contributing to the Cu $3d$ spectral weight.

proximation is certainly valid. In optimizing the parameter values, we note that (a) E_{gap} is determined by $\Delta_{pd}-T_{pp}$, (b) the energy difference between peaks B (3.1 eV) and E (12.3 eV) is primarily determined by Racah $A-\Delta_{pd}$, (c) the weight of the d^8 structure, relative to that of the $d^9\underline{L}$ structure, is determined mainly by $T_{pd}(b_1)$, and (d) the shape of the $d^9\underline{L}$ structure (including shoulder C at 4.8 eV) is influenced by T_{pp}. Within the criteria mentioned above [(a)–(c)], the difference between the positions of peak D_1 (8.8 eV) and D_2 (10.0 eV) turns out to be a little too large as a result of the mixing of the d^8 and $d^{10}\underline{L}^2$ final states. This problem is absent when using an impurity approach, where an O $2p$ band is used instead of a set of five discrete levels, resulting in a broader $d^{10}\underline{L}^2$ final state.

Peak F (16.2 eV), which is a $^1A_1$ state derived from the free-atom ^1S state at the extreme high-energy side of the spectrum, has subsequently been observed at 70–74 eV photon energies as shown in Fig. 4.

The first ionization state can be found at shoulder A (1.2 eV). This state is identified to have $^1A_1$ symmetry:

$$|\psi\rangle=\sqrt{0.64}|d^9\underline{L},b_1b_1\rangle+\sqrt{0.28}|d^{10}\underline{L}^2,b_1b_1\rangle+\sqrt{0.07}|d^8,b_1b_1\rangle \quad (17)$$

plus less than 1% of states having a_1a_1, b_2b_2 and ee character. This is consistent with recent calculations using an Anderson impurity description.[23] The second ionization state has a $^3B_1$ symmetry with energy 2.7 eV. The energy separation of 1.5 eV between these two states, which can be interpreted as an estimate of a ligand hole–Cu d hole exchange interaction, is several times larger than in those impurity calculations, due to the discreteness of the ligand hole states. A more formal definition of exchange is the difference in energy between the $^1A_1$ and $^3A_1$ lowest-lying states which is even larger (3.4 eV).

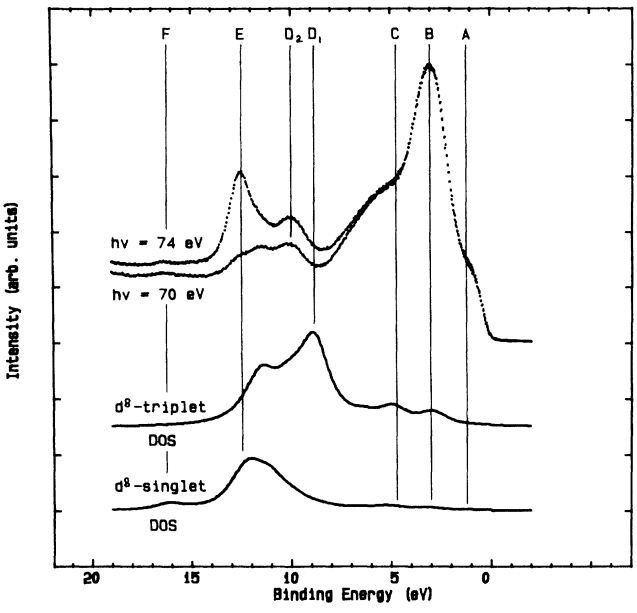

FIG. 4. Valence-band Cu $3p$ resonant photoemission of CuO, normalized to the peak height. The upper dotted line shows the experimental spectrum at the Cu $3p$ resonance ($h\nu=74$ eV) and the lower dotted line out of resonance ($h\nu=70$ eV). The upper solid line is the calculated Cu $3d^8$-triplet DOS and the lower solid line the Cu $3d^8$-singlet DOS, using the cluster-model theory for parameter values as in Figs. 2 and 3.

Figure 4 shows the Cu $3p$ resonant photoemission of the CuO valence band. The emission is at resonance for $h\nu=74$ eV and off resonance for $h\nu=70$ eV. The resonance process probes the Cu d^8 final states and involves Auger matrix elements of the Coulomb interaction, which causes a d^{10}-to-d^8 Koster-Kronig decay.[51,78,79] Figure 4 also shows the calculated d^8 DOS, split up into a singlet and a triplet contribution, using the same parameter values as in Figs. 2 and 3. A comparison between experiment and theory reveals that the energy positions of the d^8 final states are well predicted by the theory. Also the observation that the singlets (especially ^1G) resonate more strongly than the triplets, is expected since the Auger matrix element for the ^1G states in Cu LVV Auger spectra is by far the largest.[80]

B. One-particle calculations

The analysis given above, and that by Ghijsen *et al.*,[14] have established that cluster calculations provide a better description of the overall electronic structure of CuO than band-structure calculations with regard to the band gap, the local magnetic moment, and the complete one-electron removal spectrum. In a band-structure calculation the total wave function is a mathematical tool used to describe the ground-state electron density and total energy, and therefore is conveniently chosen to be a single Slater determinant of one-particle Bloch wave functions. This means that the effects of electron correlation are only present in the ground-state energy and electron density via an effective one-particle potential and not in the wave function. Therefore we expect that the density of states obtained from these one-particle energies should coincide with that of the cluster calculation without Coulomb interactions. Figure 5 shows the calculated d and p spectral weight using the same parameter values as in Figs. 2, 3, and 4, but with the Racah parameters $A=B=C=0$. It also shows the results obtained from local-density approximation (LDA) band-structure calculations by Czyzyk.[14] The striking similarity in the results for the d spectral weight indicates that for an energy scale of larger than about 0.5 eV the influence of the nearest neighbors on the electronic structure dominates over that of the rest of the lattice. There are also similarities to be seen in the results for the p spectral weight, but more differences can be noticed. This can be understood from the fact that the oxygen states are expected to delocalize to form a band and that the nearest-neighbor coordination for oxygen is not taken into account properly in the cluster chosen.

C. Optical spectra

The energies for local optical transitions can be found from the one-particle energy-level scheme in Fig. 2. Us-

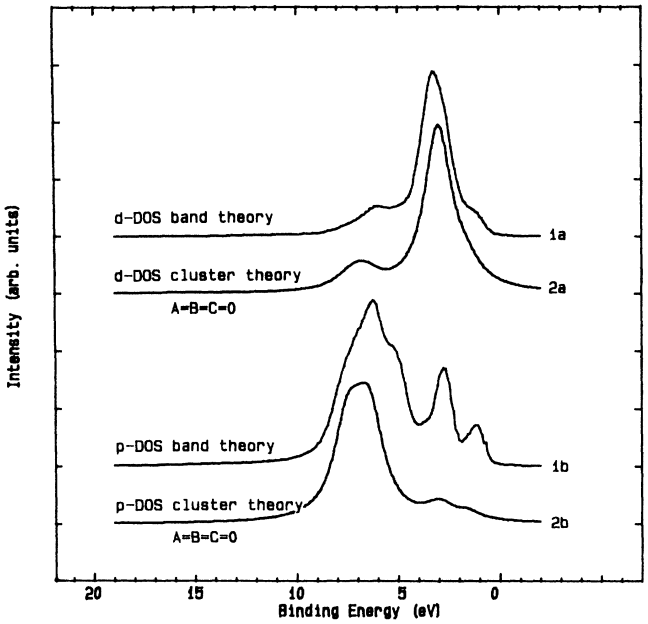

FIG. 5. One particle theoretical calculations of the CuO valence-band DOS. Line 1*a* shows the Cu 3*d* partial DOS and 1*b* the O 2*p* partial DOS as obtained from band-structure calculations by Czyzyk.[14] Line 2*a* shows the Cu 3*d* partial DOS and 2*b* the O 2*p* partial DOS as obtained from the cluster-model theory, where the Racah *A*, *B*, and *C* parameters are set to zero, which is equivalent to the one-hole problem. Other parameters in the cluster-model theory are the same as in the calculations for Figs. 2, 3, and 4. Lines 1*a* and 1*b* are shifted 0.8 eV towards higher binding energies, and lines 2*a* and 2*b* 1.6 eV, as to aline the main structure to that of the experimental valence-band photoemission spectra.

ing parameter values obtained above, the local *d*-*d* optical transitions occur at 1.3, 1.4, and 1.5 eV photon energies. These transitions are electric dipole forbidden and therefore weak, and can only be observed if they fall in the band gap. Both the intensities and energies are in strong disagreement with the assignments by Geserich *et al.*[81]

The local charge-transfer optical transitions to bonding O 2*p*-ligand orbitals are also forbidden. The transition to nonbonding orbitals are allowed and occur between 3.5 and 6.0 eV. However, these energies are well beyond the band-gap transition, which will dominate the optical absorption.

The band-gap transition itself is a *non*local charge-transfer transition. To simulate it, we would need to start with a minimum of two clusters in the ground-state configuration, and we would end up with one of them in the full Cu 3*d*–O 2*p* shell configuration, and the other in a two-hole configuration. The transition energy (1.4 eV experimentally and 1.8 eV in this cluster calculation) is much lower than for local charge-transfer transitions because the two-hole $d^9\underline{L}$ final state is allowed to hybridize with the higher-lying $d^{10}\underline{L}^2$ and d^8 final states as to form the ${}^1A_1$ first ionization state described above.

D. Parameters sensitivity

From the calculations presented above, we find that the Racah *A* parameter is between 6 and 7 eV, Δ_{pd} between 2 and 3.5 eV, $T_{pd}(b_1)$ between 2 and 3 eV, and T_{pp} between 0.5 and 1.5 eV. The uncertainties in Δ_{pd} and T_{pp} are relatively large, but their difference $\Delta_{pd}-T_{pp}$ is determined by $E_{\rm gap}=1.8$ eV.

In order to study the sensitivity to $E_{\rm gap}$, we calculate the *d* spectral weight also for $E_{\rm gap}=1.2$ and 2.4 eV, which are shown in Fig. 6 and Table II. The results reveal that a reliable set of parameter values cannot be obtained from *d* spectral weight data alone, because these are rather similar for three largely different band-gap values. Instead the band-gap value will be needed too as an input.

In Table IV we list some results obtained by others. From Cu $2p_{3/2}$ core level spectroscopy, Ghijsen *et al.*[14] have calculated the charge-transfer energy Δ, the transfer integral *T*, and the average ground-state *d*-hole occupation $\langle n_d \rangle$, using a simple two-level cluster approach as applied previously for the copper and nickel dihalides.[82–84] Shen *et al.*[45] have carried out a similar analysis based on both Cu $2p_{3/2}$ core level as well as valence-band spectroscopy.

E. The electronic structure of the high-T_c compounds

To get an estimate of the influence of the out-of-plane (apex) oxygen atoms on the electronic structure of high-T_c compounds, we repeat the same calculation for a $(CuO_6)^{10-}$ cluster in D_{4h} symmetry. The set of CuO_4 cluster orbitals is then extended with one ligand O 2*p* or-

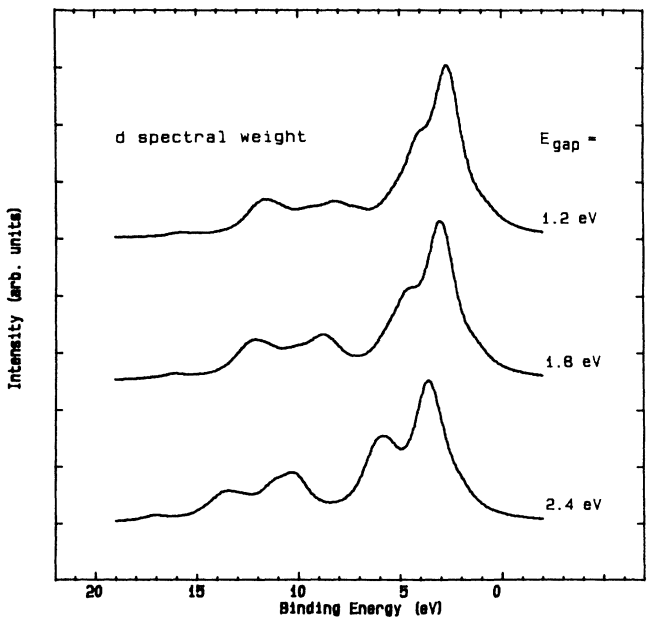

FIG. 6. Calculated Cu 3*d* spectral weight of CuO, for three different energy gaps (1.2, 1.8, and 2.4 eV). The three sets of parameter values used in the cluster-model calculations are listed in Table II.

TABLE IV. Comparison of parameter values obtained from various methods.

This work	Ghijsen *et al.*	Shen *et al.*
E_{gap} 1.8 eV		$E_{gap}=1.3$ eV
$\Delta_{pd}-T_{pp}=1.75$ eV	$\Delta=1.55$ eV	$\Delta=1.0$ eV
$T_{pd}=2.5$ eV	$T=2.5$ eV	$T=2.4$ eV
$U(^1G)=A+4B+2C=7.76$ eV		$U=7.3$ eV
$\langle n_d\rangle=0.665$	$\langle n_d\rangle=0.65$	$\langle n_d\rangle=0.60$

bital with a_1 symmetry and two with e symmetry. Their energies and transfer integrals are listed in Table V. The nonbonding orbitals are not considered as they do not influence the d emission. We calculate the d spectral weight, using the same parameters as for CuO and assuming the same energies for the apex oxygen (Δ_{pd}^{apex}) as for the in-plane oxygens (Δ_{pd}). We have taken the in-plane Cu–O distances (d_{plane}) to be 1.89 Å and the apex Cu–O distances (d_{apex}) 2.41 Å, which are the values for La_2CuO_4, and applied Harrison's relationship[85] that the $3d$-$2p$ and $2p$-$2p$ transfer integrals are proportional to the distance to the power -3.5 and -2, respectively. In Fig. 7 the result is compared to the $(CuO_4)^{6-}$ cluster result for CuO. It shows that with the same set of parameters, the influence of the apex oxygens on the overall shape of the d spectral weight is very small.

To be more specific, we also investigate this influence on the nature of the first ionization states, which will have a singlet ($^1A_1$) or triplet ($^3B_1$) character. Using again the same set of parameters as in Fig. 7, we vary the apex relative to the in-plane Cu–O distance and calculate the energy difference between the $^1A_1$ and the $^3B_1$ states closest to the Fermi level. Figure 8 shows that as long as the ratio between the apex versus the in-plane Cu–O distances is larger than 1.06 (a Cu–O distance of 2.0 Å), the first ionization state will have singlet character. In O_h symmetry, the triplet is lowest in energy, but the singlet-triplet energy difference is small (-0.35 eV) and is totally due to the multiplet splitting in d^8. This difference in energy has the opposite sign and is much larger for the CuO_6 cluster with La_2CuO_4 distances (0.7 eV) as well as the CuO_4 cluster (1.5 eV) due to the lower symmetry causing differences in hybridization for a_1 and b_1 symmetry. As the energies of the apex oxygens are not known precisely, we carry out the same analysis for varying apex oxygen energies with the same set of parameters, but now with the apex-in-plane Cu–O distance ratio fixed to the La_2CuO_4 value. From Fig. 9 it can be seen that again the first ionization state will have singlet rather than triplet character provided that the energy difference between the apex and in-plane oxygen orbitals ($\Delta_{pd}-\Delta_{pd}^{apex}$) does not exceed 1.7 eV (the apex oxygen level being closer to the Fermi level). Note that for energy differences larger than 3.4 eV, the ground state will no longer consist of a hole mainly in a Cu $3d_{x^2-y^2}$ orbital, but rather in an apex oxy-

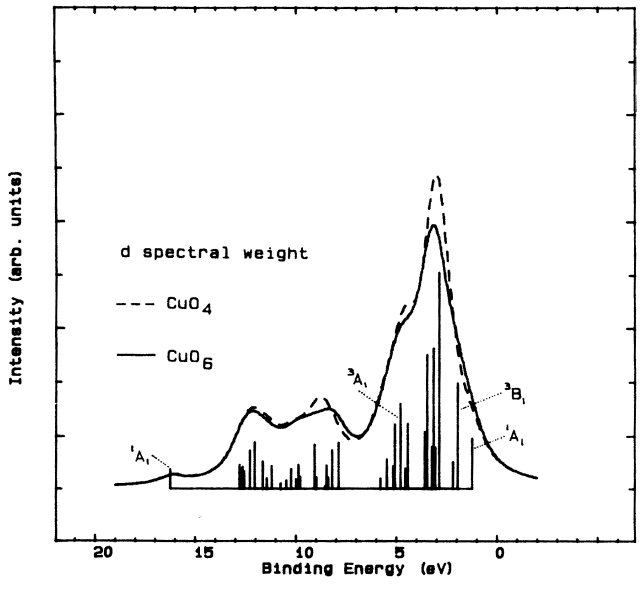

FIG. 7. Calculated Cu $3d$ spectral weight of a $(CuO_4)^{6-}$ cluster (dashed line) and a $(CuO_6)^{10-}$ cluster (solid line). The parameter values used are the same as in Figs. 2, 3, and 4. In addition, for the $(CuO_6)^{10-}$ cluster, $\Delta_{pd}^{apex}=\Delta_{pd}$ and d_{apex}/d_{plane} = 2.41 Å/189 Å. Also shown are the unbroadened states contributing to the Cu $3d$ spectral weight of the $(CuO_6)^{10-}$ cluster.

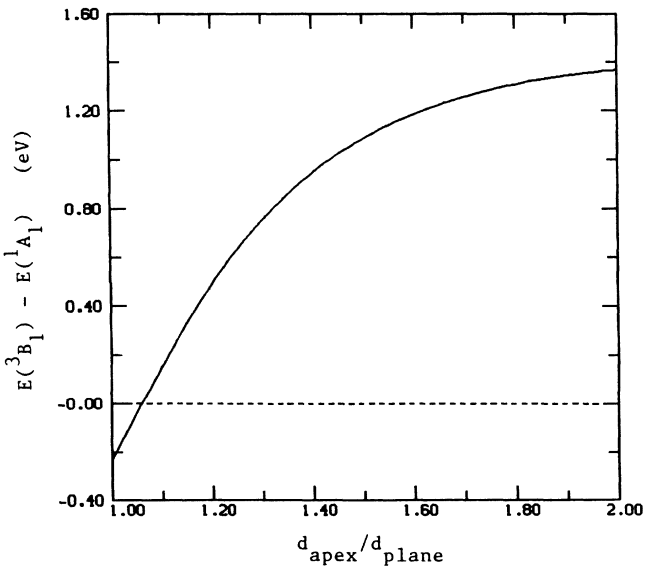

FIG. 8. Calculated energy difference between the $^3B_1$ and $^1A_1$ states closest to the Fermi level for a $(CuO_6)^{10-}$ cluster as a function of d_{apex}/d_{plane}. The parameter values used are otherwise the same as in Fig. 7.

TABLE V. A $(CuO_6)^{10-}$ cluster extension to the one-hole basis functions and matrix elements for the $(CuO_4)^{6-}$ cluster in D_{4h} symmetry as previously shown in Table I and Fig. 1. The added apex oxygens are numbered with 5 and 6. The nonbonding ligand O $2p$ orbitals are not included.

Irreducible representations m	O $2p$ basis p_m^{apex}
a_1	$(1/\sqrt{2})(p_{z_5}-p_{z_6})$
e	$(1/\sqrt{2})(p_{x_6}-p_{x_5}),(1/\sqrt{2})(p_{y_6}-p_{y_5})$

Irreducible representations m	Matrix elements $\langle p_m^{\text{apex}}\|H\|p_m^{\text{apex}}\rangle$	$\langle p_m^{\text{apex}}\|H\|p_m\rangle$	$\langle p_m^{\text{apex}}\|H\|d_m\rangle$
a_1	$\Delta_{pd}^{\text{apex}}$	$-\sqrt{2}T_{pp}4\left[\frac{d_{\text{plane}}}{d_{\text{apex}}}\right]^3\Big/\left[1+\left[\frac{d_{\text{plane}}}{d_{\text{apex}}}\right]^2\right]^2$	$\left[\frac{d_{\text{plane}}}{d_{\text{apex}}}\right]^{3.5}\sqrt{2}T_{pd}(b_1)\Big/\sqrt{3}$
e	$\Delta_{pd}^{\text{apex}}$	$T_{pp}4\left[\frac{d_{\text{plane}}}{d_{\text{apex}}}\right]^3\Big/\left[1+\left[\frac{d_{\text{plane}}}{d_{\text{apex}}}\right]^2\right]^2$	$\left[\frac{d_{\text{plane}}}{d_{\text{apex}}}\right]^{3.5}T_{pd}(b_1)\Big/2\sqrt{2}$

gen orbital of a_1 symmetry.

It is expected that the same results will be obtained for other high-T_c compounds consisting of pyramidal $(CuO_5)^{8-}$ clusters. It might be expected that the influence of the apex oxygen atoms is a bit larger because they are closer to the CuO_4 plane, but this influence is also reduced by a factor of $\sqrt{2}$ as there is only one (instead of two) apex oxygen per cluster. This is in good agreement with the results obtained by Fujimori,[20] who also found a value of 1.7 eV for the on-site energy difference between the apex and in-plane oxygens as the crossing point for the triplet or the singlet to be the first ionization state.

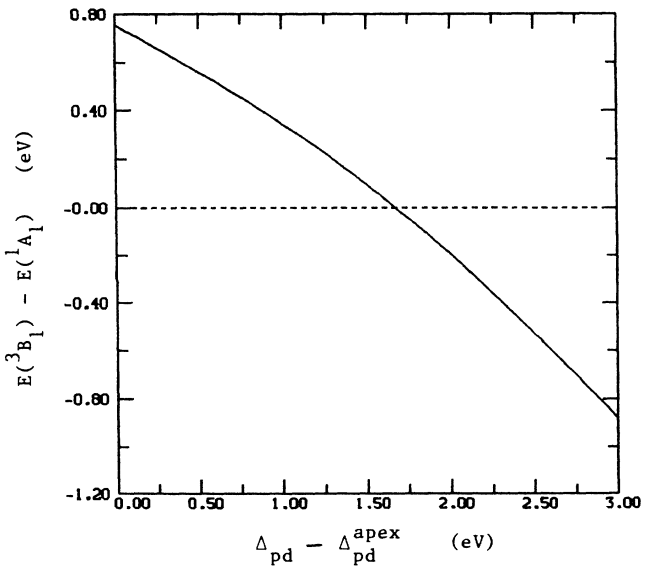

FIG. 9. Calculated energy difference between the $^3B_1$ and $^1A_1$ states closest to the Fermi level for a $(CuO_6)^{10-}$ cluster as a function of $\Delta_{pd}-\Delta_{pd}^{\text{apex}}$. The parameter values used are otherwise the same as in Fig. 7.

IV. CONCLUSIONS

The cluster-model calculations give a good quantitative understanding of the electronic structure of CuO. In particular, the band gap, the intensities, and positions of the d^8 and $d^9\underline{L}$ structures are well reproduced. The breaking of the translational symmetry is found to introduce only minor errors in the Cu $3d$ spectral weight in the 2–7 eV binding-energy range. CuO and the high-T_c superconducting copper oxide materials are highly correlated systems, in spite of the fact that the Cu $3d$–O $2p$ hybridization is extremely large. The band gap is caused by electron correlation, but is of the charge-transfer type. The first ionization state in CuO and the additional holes in the superconducting copper oxides are primarily of O $2p$ character which in the configuration-interaction approach is a state of primarily $d^9\underline{L}$ character, having a $^1A_1$ symmetry, because of a strong antiferromagnetic exchange interaction (3.4 eV) of the O $2p$ ligand hole with the Cu $3d$ hole. This state will have $^3B_1$ symmetry only when the apex oxygen $2p$ states are closer to the Fermi level by more than 1.7 eV than those of the in-plane oxygens, or when the ratio between the apex versus the in-plane Cu–O distances is smaller than 1.06. The d-d optical transitions are predicted to be clustered around 1.4 ± 0.1 eV, quite contrary to published assignments.[81]

ACKNOWLEDGMENTS

This work was supported by the Netherlands Foundation for Fundamental Research on Matter (FOM), the Netherlands Foundation for Chemical Research (SON), and the Netherlands Organization for the Advancement of Pure Research (NWO).

APPENDIX

In solving the two-hole Green's-function problem [Eqs. (10)–(16)], we treat the d-d Coulomb and exchange interactions H_1 as perturbation to the one-particle H_0, as it

has been done in the Cini-Sawatzky theory[86–88] for Auger spectroscopy. We write then the exact expressions:

$$G(z)=G_0(z)+G_0(z)T(z)G_0(z) \tag{A1}$$

$$T(z)=H_1+H_1G_0(z)T(z) \tag{A2}$$

where

$$G_0(z)=(z+\delta-H_0)^{-1}\ . \tag{A3}$$

From that theory, the uncorrelated two-hole Green's function can be obtained by convoluting the single-hole Green's functions

$$g^{st}_{qr}(m,n,z)=\frac{1}{2\pi i}\int_{-\infty}^{\infty} g^s_q(m,z-\zeta)g^t_r(n,\zeta)d\zeta \tag{A4}$$

with the definitions

$$g^{st}_{qr}(m,n,z)=\langle 0|q_m r_n G_0(z)t^\dagger_n s^\dagger_m|0\rangle \tag{A5}$$

$$g^s_q(m,z)=\langle 0|q_m G_0(z)s^\dagger_m|0\rangle \tag{A6}$$

$$g^t_r(n,z)=\langle 0|r_n G_0(z)t^\dagger_n|0\rangle \tag{A7}$$

and where the operators q, r, s, and t denote the operators d, p, a, or b. Because H_1 only couples two d-hole states, all T-matrix elements are zero except

$$T^{m'n'}_{mn}(\Gamma,z)=\langle 0|d_m d_n T(\Gamma,z)d^\dagger_{n'}d^\dagger_{m'}|0\rangle\ . \tag{A8}$$

Here $d^\dagger_{n'}d^\dagger_{m'}|0\rangle$ and $d^\dagger_n d^\dagger_m|0\rangle$ belong, because of group theory, to the same two d-hole irreducible representations Γ in D_{4h} point group, as listed in Table III.

Making use of (A1)–(A8) we have

$$G^<_{dd}(m,m',z)=\delta_{mm'}G^<_{dd}(m,m,z) \tag{A9}$$

and

$$\begin{aligned}G^<_{dd}(m,m,z)=&\sum_\Gamma |\langle b^\uparrow_1 m|\}\Gamma\rangle|^2 G_{dd}(m,m,z,\Gamma)\\&+\delta_{mb^\uparrow_1}G^<_{dd}(b^\uparrow_1,b^\uparrow_1,z,{}^3A_1)\\&+\delta_{mb^\downarrow_1}G^<_{dd}(b^\downarrow_1,b^\downarrow_1,z,{}^3A_1)\\&+\delta_{mb^\downarrow_1}G^<_{dd}(b^\downarrow_1,b^\downarrow_1,z,{}^1A_1)\ ,\end{aligned} \tag{A10}$$

where the summation over Γ excludes ${}^1A_1$ (and ${}^3A_1$), $|\langle b^\uparrow_1 m|\}\Gamma|^2$ denotes the fractional parentage for two holes starting from a $b^\uparrow_1$ hole listed in Table VI, and

TABLE VI. Coefficients of fractional parentage $|\langle b^\uparrow_1|\}\Gamma\rangle|^2$ for two holes, starting from a b_1 spin-up hole. Γ is the irreducible representation spanned by two holes, m is the irreducible representation spanned by one hole, and ↑ or ↓ indicates spin up or down, respectively. The ${}^3A_1$ and ${}^1A_1$ are treated separately.

Γ	${}^3B_1$	${}^3A_2$	${}^3E$	${}^1B_1$	${}^1A_2$	${}^1E$
m						
$a^\uparrow_1$	1					
$a^\downarrow_1$	$\frac{1}{2}$			$\frac{1}{2}$		
$b^\uparrow_2$		1				
$b^\downarrow_2$		$\frac{1}{2}$			$\frac{1}{2}$	
$e^\uparrow$			2			
$e^\downarrow$			1			1

$$G^<_{dd}(m,m,z,\Gamma)=g^{ad}_{ad}(b^\uparrow_1,m,z)+\langle n_d\rangle g^{ad}_{ad}(b^\uparrow_1,m,z)T^{b^\uparrow_1 m}_{b^\uparrow_1 m}\times(\Gamma,z)g^{ad}_{ad}(b^\uparrow_1,m,z) \tag{A11}$$

$$G^<_{dd}(b^\uparrow_1,b^\uparrow_1,z,{}^3A_1)=(1-\langle n_d\rangle)g^{ab}_{ab}(b^\uparrow_1,b^\uparrow_1,z) \tag{A12}$$

$$G^<_{dd}(b^\downarrow_1,b^\downarrow_1,z,{}^3A_1)=\tfrac{1}{2}G^<_{dd}(b^\uparrow_1,b^\uparrow_1,z,{}^3A_1) \tag{A13}$$

$$\begin{aligned}G^<_{dd}(b^\downarrow_1,b^\downarrow_1,z,{}^1A_1)=&-G^<_{dd}(b^\downarrow_1,b^\downarrow_1,z,{}^3A_1)+g^{ad}_{ad}(b^\uparrow_1,b^\uparrow_1,z)\\&+\langle n_d\rangle g^{ad}_{ad}(b^\uparrow_1,b^\uparrow_1,z)T^{b^\uparrow_1 b^\uparrow_1}_{b^\uparrow_1 b^\uparrow_1}\\&\times({}^1A_1,z)g^{ad}_{ad}(b^\uparrow_1,b^\uparrow_1,z)\ .\end{aligned} \tag{A14}$$

Note that we have treated ${}^3A_1$ and ${}^1A_1$ separately because the Pauli's exclusion principle as we started with a $b^\uparrow_1$ hole already present. Similar expressions can be derived for the p spectral weight.

We also have, where Γ now also includes ${}^1A_1$,

$$\begin{aligned}G^<_{d^8}(m,n,z)=&g^{dd}_{dd}(m,n,z)\\&+g^{dd}_{dd}(m,n,z)T^{mn}_{mn}(\Gamma,z)g^{dd}_{dd}(m,n,z)\ .\end{aligned} \tag{A15}$$

The T-matrix elements can be found by solving the system of linear equations:

$$\begin{aligned}T^{mn}_{mn}(\Gamma,z)=&U(m,m,n,n)\\&+\sum_{m'n'}U(m,m',n,n')\\&\times g^{dd}_{dd}(m',n',z)T^{mn}_{m'n'}(\Gamma,z)\ .\end{aligned} \tag{A16}$$

[1] L. F. Mattheis, Phys. Rev. Lett. **58**, 1028 (1987).

[2] A. T. Park, K. Terakura, T. Oguchi, A. Yanase, and M. Ikeda, Technical Report ISSN Ser. A. 1960 (1988).

[3] J. Zaanen, G. Jepsen, O. Gunnarson, A. T. Paxton, O. K. Anderson, and S. A. Svane, Proceedings of the International Conference on High T_c Superconductors and Mechanisms of Superconductivity, Interlaken, 1988 [Physica **153-155C**, 1636 (1988)].

[4] J. Yu, A. J. Freeman, and J. H. Xu, Phys. Rev. Lett. **58**, 1035 (1987).

[5] S. Massida, J. Yu, and A. J. Freeman, Physica C **152**, 251 (1988).

[6] F. Herman, R. V. Kasowski, and W. Y. Hsu, Phys. Rev. B **36**, 6904 (1987).

[7] F. Herman, R. V. Kasowski, and W. Y. Hsu, Phys. Rev. B **38**, 204 (1988).

[8] F. Herman, R. V. Kasowski, and W. Y. Hsu, Physica C **153-155**, 629 (1988).

[9]K. Terakura, T. Oguchi, A. R. Williams, and J. Kübler, Phys. Rev. B **30**, 4734 (1984).
[10]K. Terakura, A. R. Williams, T. Oguchi, and J. Kübler, Phys. Rev. Lett. **52**, 1830 (1984).
[11]H. J. de Boer and E. J. W. Verwey, Proc. Phys. Soc. London, Sect. A **49**, 59 (1937).
[12]N. F. Mott, Proc. R. Soc. London, Ser. A **62**, 416 (1949).
[13]J. Hubbard, Proc. R. Soc. London, Ser. A **277**, 237 (1964).
[14]J. Ghijsen, L. H. Tjeng, J. van Elp, H. Eskes, J. Westerink, G. A. Sawatzky, and M. T. Czyzyk, Phys. Rev. B **38**, 11 322 (1988).
[15]A. Fujimori and F. Minami, Phys. Rev. B **30**, 957 (1984).
[16]A. Fujimori, F. Minami, and S. Sugano, Phys. Rev. B **29**, 5225 (1984).
[17]G. A. Sawatzky and J. W. Allen, Phys. Rev. Lett. **53**, 2339 (1984).
[18]J. Zaanen, G. A. Sawatzky, and J. W. Allen, Phys. Rev. Lett. **55**, 418 (1985).
[19]J. Zaanen, Ph.D. thesis, University of Groningen, 1986.
[20]A. Fujimori, Phys. Rev. B **39**, 793 (1989).
[21]F. Mila, Phys. Rev. B **38**, 11 358 (1988).
[22]A. K. McMahan, R. M. Martin, and S. Satpathy, Phys. Rev. B **38**, 6650 (1988).
[23]H. Eskes and G. A. Sawatzky, Phys. Rev. Lett. **61**, 1415 (1988).
[24]G. A. Sawatzky, in *Proceedings of the Adriatico Research Conference on the Theoretical Understanding of High T_c Superconductors, Trieste, 1988,* edited by S. Lundqvist, E. Tosatti, M. P. Tosi, and Yu Lu (World Scientific, Singapore, 1989), p. 243.
[25]H. Eskes, L. H. Tjeng, G. A. Sawatzky, in *Mechanisms of High-Temperature Superconductivity,* Proceedings of the NEC Symposium, Hakone, Tokyo, 1988, edited by H. Kamimura and A. Ofhiyama (Springer, Berlin, 1989).
[26]G. Wendin, J. Phys. Colloq. **48**, 1157 (1987).
[27]J. C. Fuggle, J. Fink, and N. Nücker, in *Mechanisms of High-Temperature Superconductivity,* Proceedings of the International Conference on High T_c Superconductivity, Trieste, 1988, edited by H. Kamimura and A. Oshiyama (Springer-Verlag, Berlin, 1989), p. 20.
[28]T. Takahashi, F. Maeda, S. Hosoya,and M. Sato, Jpn. J. Appl. Phys. **26**, L349 (1987).
[29]T. Takahashi, F. Maeda, H. Katayama-Yoshida, Y. Okabe, T. Suzuki, A. Fujimori, S. Hosoya, S. Shamoto, and M. Sato, Phys. Rev. B **37**, 9788 (1988).
[30]P. D. Johnson, S. L. Qiu, L. Jiang, M. W. Ruckman, M. Strongin, S. L. Hubert, R. F. Garrett, B. Sinkovic, N. V. Smith, R. J. Cava, C. S. Jee, D. Nichols, E. Kaczanowicz, R. E. Salomon, and J. E. Crow, Phys. Rev. B **35**, 8811 (1987).
[31]J. A. Yarmoff, D. R. Clarke, W. Drube, U. O. Karlsson, A. Taleb-Ibrahimi, and F. J. Himpsel, Phys. Rev. B **36**, 3967 (1987).
[32]N. G. Stoffel, J. M. Tarascon, Y. Chang, M. Onellion, D. W. Niles, and G. Margaritondo, Phys. Rev. B **36**, 3986 (1987).
[33]E. R. Moog, S. D. Bader, A. J. Arko, and B. K. Flandermeyer, Phys. Rev. B **36**, 5583 (1987).
[34]T. Takahashi, F. Maeda, H. Arai, H. Katayama-Yoshida, Y. Okabe, T. Suzuki, S. Hosoya, A. Fujimori, T. Shidara, T. Koide, T. Miyahara, M. Onoda, S. Shamoto, and M. Sato, Phys. Rev. B **36**, 5686 (1987).
[35]P. Thiry, G. Rossi, Y. Petroff, A. Revcolevschi, and J. Jegoudez, Europhys. Lett. **5**, 55 (1988).
[36]N. G. Stoffel, Y. Chang, M. K. Kelly, L. Dottl, M. Onellion, P. A. Morris, W. A. Bonner, and G. Margaritondo, Phys. Rev. B **37**, 7952 (1988).
[37]A. Samsavar, T. Miller, T.-C. Chiang, B. G. Pazol, T. A. Friedmann, and D. M. Ginsberg, Phys. Rev. B **37**, 5164 (1988).
[38]R. S. List, A. J. Arko, Z. Fisk, S.-W. Cheong, J. D. Thompson, J. A. O'Rourke, C. G. Olson, A.-B. Yang, T.-W. Pi, J. E. Schirber, and N. D. Shinn, J. Magn. Magn. Mater. **75**, L1 (1988).
[39]A. J. Arko, R. S. List, Z. Fisk, S.-W. Cheong, J. D. Thompson, J. A. Rourke, C. G. Olson, A.-B. Yang, T.-W. Pi, J. E. Schirber, and N. D. Shinn, Phys. Rev. B **38**, 11 966 (1988).
[40]M. Onellion, Ming Tang, Y. Chang, G. Margaritondo, J. M. Tarascon, P. A. Morris, W. A. Bonner, and N. G. Stoffel, Phys. Rev. B **38**, 881 (1988).
[41]T. Takahashi, M. Matsuyama, H. Katayama-Yoshida, Y. Okabe, S. Hosoya, K. Seki, H. Fujimoto, M. Sato, and H. Inokuchi, Nature **334**, 691 (1988).
[42]A. Fujimori, E. Takayama-Muromachi, Y. Uchida, and B. Okai, Phys. Rev. B **35**, 8814 (1987).
[43]A. Fujimori, E. Takayama, and Y. Uchida, Solid State Commun. **63**, 857 (1987).
[44]A. Bianconi, A. Congiu Castellano, M. de Santis, P. Delogu, A. Gargano, and R. Giorgi, Solid State Commun. **63**, 1135 (1987).
[45]Z.-X. Shen, J. W. Allen, J. J. Yeh, J.-S. Kang, W. Ellis, W. Spicer, I. Lindau, M. B. Maple, Y. D. Dalichaouch, M. S. Torikachvili, J. Z. Sun, and T. H. Geballe, Phys. Rev. B **36**, 8414 (1987).
[46]J. C. Fuggle, P. J. W. Weijs, R. Schoorl, G. A. Sawatzky, J. Fink, N. Nücker, P. J. Durham, and W. M. Temmerman, Phys. Rev. B **37**, 123 (1988).
[47]D. van der Marel, J. van Elp, G. A. Sawatzky, and D. Heitmann, Phys. Rev. B **37**, 5136 (1988).
[48]P. Steiner, S. Hüfner, V. Kinsinger, I. Sander, B. Siegwart, H. Schmitt, R. Schulze, S. Junk, G. Schwitzgebel, A. Gold, G. Politis, H. P. Müller, R. Hoppe, S. Kemmler-Sack, and C. Kunz, Z. Phys. B **69**, 449 (1988).
[49]R. L. Kurtz and R. L. Stockbauer, Phys. Rev. B **35**, 8818 (1987).
[50]M. Onellion, Y. Chang, D. W. Niles, R. Joynt, G. Margaritondo, N. G. Stoffel, and J. M. Tarascon, Phys. Rev. B **36**, 819 (1987).
[51]M. R. Thuler, R. L. Benbow, and Z. Hurych, Phys. Rev. B **26**, 669 (1982).
[52]M. Grioni, R. Schoorl, J. B. Goedkoop, J. C. Fuggle, F. Schäfers, E. E. Koch, G. Rossi, J.-M. Esteva, and R. Karnatak, Phys. Rev. B **39**, 1541 (1989).
[53]F. P. Koffyberg and F. A. Benko, J. Appl. Phys. **53**, 1173 (1982).
[54]B. T. Thole (private communication).
[55]S. Åsbrink and L. J. Norrby, Acta Crystallogr. Sect. B **26**, 8 (1970).
[56]G. Shirane, Y. Endoh, R. J. Birgenau, M. A. Kastner, Y. Hidaka, M. Oda, M. Suzuki, and T. Murakami, Phys. Rev. Lett. **59**, 1613 (1987).
[57]B. X. Yang, J. M. Tranquada, and G. Shirane, Phys. Rev. B **38**, 174 (1988).
[58]B. X. Yang, T. R. Thurston, J. M. Tranquada, and G. Shirane, Phys. Rev. B **39**, 4343 (1989).
[59]J. B. Forsyth, P. J. Brown, and B. M. Wanklin, J. Phys. C **21**, 2917 (1988).
[60]S. Sugai, S.-I. Shamoto, and M. Sato, Phys. Rev. B **38**, 6436 (1988).
[61]J. B. Goodenough, Phys. Rev. B **100**, 564 (1955).

[62]J. B. Goodenough, J. Phys. Chem. Solids **6**, 287 (1958).
[63]J. Kanamori, J. Phys. Chem. Solids **10**, 87 (1959).
[64]J. C. Slater, *Quantum Theory of Atomic Structure* (McGraw-Hill, New York, 1960), Vols. 1 and 2.
[65]J. S. Griffith, *The Theory of Transition Metal Ions* (Cambridge University Press, Cambridge, 1961).
[66]D. van der Marel and G. A. Sawatzky, Phys. Rev. B **37**, 10 674 (1988).
[67]G. J. M. Janssen and W. C. Nieuwpoort, Phys. Rev. B **38**, 3449 (1988).
[68]G. Aissing, Ph.D. thesis, University of Groningen, 1988 (unpublished).
[69]N. Nücker, J. Fink, J. C. Fuggle, P. J. Durham, and W. M. Temmerman, Phys. Rev. B **37**, 5158 (1988).
[70]N. Nücker, J. Fink, J. C. Fuggle, P. J. Durham, and W. M. Temmerman, Physica C **153–155**, 119 (1988).
[71]P. Kuiper, G. Kruizinga, J. Ghijsen, M. Grioni, P. J. W. Weijs, F. M. F. de Groot, G. A. Sawatzky, H. Verweij, L. F. Feiner, and H. Petersen, Phys. Rev. B **38**, 6483 (1988).
[72]A. Bianconi, A. Congiu Castellano, M. de Santis, P. Rudolf, P. Lagarde, A. M. Flank, and A. Marcelli, Solid State Commun. **63**, 1009 (1987).
[73]F. J. Himpsel, G. V. Chandrashekhar, A. B. McLean, and M. W. Shäfer, Phys. Rev. B **38**, 11 946 (1988).
[74]J. C. Slater and G. F. Koster, Phys. Rev. **94**, 1498 (1954).
[75]L. F. Mattheiss, Phys. Rev. B **5**, 290 (1972).
[76]C. E. Moore, *Atomic Energy Levels,* Natl. Bur. Stand. (U.S.) Circ. No. 467 (U.S. GPO, Washington, D.C., 1958), Vols. 1–3.
[77]J. J. Yeh and I. Lindau, At. Data Nucl. Data Tables **32**, 1 (1985).
[78]L. A. Feldkamp and L. C. Davis, Phys. Rev. Lett. **43**, 151 (1979).
[79]T. Ishii, M. Taniguchi, A. Kakizaki, K. Naito, H. Sugawara, and I. Nagakura, Phys. Rev. B **33**, 5664 (1986).
[80]E. Antonides, E. C. Janse, and G. A. Sawatzky, Phys. Rev. B **15**, 1669 (1977).
[81]H. P. Geserich, G. Scheiber, J. Geerk, H. C. Li, G. Linker, W. Assmus, and W. Weber, Europhys. Lett. **6**, 277 (1988).
[82]G. van der Laan, C. Westra, C. Haas, and G. A. Sawatzky, Phys. Rev. B **23**, 4369 (1981).
[83]G. van der Laan, Solid State Commun. **42**, 165 (1982).
[84]J. Zaanen, C. Westra, and G. A. Sawatzky, Phys. Rev. B **33**, 8060 (1986).
[85]W. A. Harrison, *Electronic Structure and the Properties of Solids* (Freeman, San Francisco, 1980).
[86]M. Cini, Solid State Commun. **24**, 681 (1977).
[87]G. A. Sawatzky, Phys. Rev. Lett. **39**, 504 (1977).
[88]V. Drchal and J. Kudrnovsky, Phys. Status Solidi B **114**, 627 (1982).